K. H. Digges, P. G. Bedewi, G. T. Bahouth, and N. E. Bedewi
FHWA/NHTSA National Crash Analysis Center, The George Washington University

J. Augenstein, E. Perdeck, and J. Stratton
William Lehman Injury Research Center, University of Miami

Determination And Modeling of Ankle Injury Causation

Abstract

A finite element model of the human lower extremity has been developed. The model accurately represents the geometry and mass of all skeletal elements. The hip, knee, and ankle joints contain the proper active and passive characteristics. These properties can be modified to evaluate different levels of muscle activation at each joint. Initial findings have shown that muscle tensioning can play a significant role on the kinematics and impact response of the ankle.

In order to explore injury mechanisms, the model is being used in conjunction with detailed crash investigations of occupants with ankle injuries. To permit reconstruction of the injury producing environment, precise measurements of the vehicle interior are made. The position of the lower limb is determined with the aid of a skeletal device adjusted to the length of the injures occupant's limb segments.

The resulting approach permits the assessment of the role of critical crash variables on ankle injuries. These variables include: muscle tensing, inertia loads from the leg and upper body, footwell acceleration; non-stable foot loading from the floor or foot pedals;

footwell, knee restraint, and seating geometry; crash severity and direction; and footwell intrusion.

Introduction

Until recently, injuries to the lower extremities have received less attention that the more life threatening injuries of the head and chest. While rarely fatal, these injuries can be very debilitating. The proposed European standard for crash testing vehicles in the frontal offset mode has greatly increased the focus of attention on ankle injuries. These tests frequently produce footwell intrusion which has been shown by Thomas and others to increase the risk of ankle injuries [1].

Studies of NASS data indicate that more than 50% of ankle and foot injury harm to drivers who are restrained occurs without any footwell intrusion [2]. This result suggests that factors other than intrusion may also play a major role in ankle injury causation.

Other factors include: muscle tensing, inertia loads from the leg and upper body, footwell acceleration; non-stable foot loading from the floor or foot pedals; footwell, knee restraint, and seating geometry; and crash severity and direction. In order to assess the complex interaction of factors which may contribute to ankle injuries, a methodology for reconstructing crash injuries has been developed. This methodology includes a detailed crash and injury investigation, followed by a reconstruction of the injury producing environment using a finite element model. This methodology has been implemented by the collaboration of the National Crash Analysis Center, and The William Lehman Injury Research Center.

The purpose of this paper is to describe the finite element model, and the methodology for crash reconstruction. Initial results of the model which show the effects of muscle tensing are included to illustrate the usefulness of the approach.

The Computer Model

Preliminary assessment of the issues surrounding lower extremity injury can be done through low level finite element modeling. A relatively simple model can be very useful for addressing joint behavior, muscle tensioning, and injury potential in a high speed impact event. Additionally, it can provide a foundation for more complex models and dictate the direction of their development. This portion of the study performed at The George Washington University focused on three topics:

1. The development of a lower extremity, finite element model with accurate joint characterization and muscle tensioning behavior
2. Performing a parametric study to determine the influence of muscle tensioning in the ankle, knee, and hip on the injury potential in the ankle.
3. Provide a basis for the development of a more complex model.

Lower extremity characterization

The lower extremity consists of three segments: the thigh, leg (often referred to as the shank or lower leg), and foot. The segments are spatially linked via several soft tissue components, most noticeably approximately 29 muscles. Most of the muscles in the leg span only one joint however several span two joints. Each of the three major joints (hip, knee, and ankle) is unique; however, all are similar in that they are each weight bearing, synovial joints surrounded by a ligamentous joint capsule [3]. Audu and Davy described the passive moments of a human joint with Equation 1 [4]:

$$M_{pass}(\theta,\dot{\theta}) = k_1 e^{-k_2(\theta-\theta_2)} - k_3 e^{-k_4(\theta_1-\theta)} - c\dot{\theta} \quad [1]$$

The *k* values are stiffness constants and depend upon the joint being modeled, *c* is the passive damping constant, and the values q1 and q2 are angles approximating the joint's limit in each direction. The composition of this equation is such that, as q reaches the joint's limit, the joint becomes extremely stiff. For joints with more than one degree-of-freedom, constants for the equation in each direction are needed. Therefore, joints such as the hip, have the passive moment described by three equations (flexion - extension, abduction - adduction, and internal - external rotation).

Subsequently, Yamaguchi determined the constants for flexion and extension in the sagittal plane for each of the joints in the lower extremity to satisfy Equation 1 [5]. These constants can be found in Table 1. Instead of modeling each active muscle individually, their overall contribution on a joint can be lumped into an active torque applied at the joint's center of rotation. Gordon *et al*. characterized this active torque in the flexion-extension modes of the lower limb joints [6]. The maximum active torques at each joint in the leg are found in Table 2.

Table 1: Passive joint moment coefficients for flexion and extension of the lower extremity.

Coefficients for Passive Joint Moment		
Ankle	K1 = 2.0 K2 = 5.0 K3 = 9.0 K4 = 5.0	C1 = .943 theta1 = 0.349 theta2 = -0.524
Knee	K1 = 3.10 K2 = 5.90 K3 = 10.5 K4 = 11.8	C1 = 3.17 theta1 = 0.00 theta2 = -1.92
Hip	K1 = 2.6 K2 = 5.8 K3 = 8.7 K4 = 1.3	C1 = 1.09 theta1 = 1.92 theta2 = -0.1744

Table 2: Active joint properties for the lower extremity in the sagittal plane.

Joint	Maximum Active Torque [N-m]	
	Extension	Flexion
Hip	-215	200
Knee	-160	80
Ankle	-125	250

Various studies have been performed to examine the impact response of the ankle and other lower limb joints. Quantities such as joint moment and joint angle can be measured and compared with injuries observed. Comparisons to the experimental data can be done with a low level FEM model, and estimates of joint failure and injury potential can be made in the post-processing analysis. For ankle injury, Begeman and Prasad determined the impact response in dorsiflexion through pendulum tests of nine sets of ankles [7]. The study indicated that injury to the ankle joint could only be directly correlated with the maximum angle of dorsiflexion. Injury could not be correlated with joint moment, pre-impact range-of-motion, or peak force values. It was determined that if the ankle exceeded 45° in dorsiflexion, injury was very likely.

Subsequent studies have indicated some inaccuracies may be present in the Begeman and Prasad methodology [8]. Most predominately, the use of limbs severed below the knee, thus removing much of the musculature responsible for resisting dorsiflexion. While it may not be reasonable to use the exact numbers put forth by Begeman and Prasad for injury potential, certain trends and relations may be observed and compared to simulation results to assess the model's performance.

Model description and impact scenario

The model created has accurate three dimensional geometry; however, the joints are restricted to motion in the sagittal plane. The focus of this model is on joint characteristics. The geometry for the finite element mesh consists of the pelvis, femur, patella, tibia, fibula, and the 26 bones of the foot. The data for the geometry is of a 50th percentile male, digitized by Viewpoint Datalabs [9]. A finite element mesh was applied to the bones and consisted of a total of 5477 thin shell elements. The mesh was then divided into four groups: the pelvis (pelvic bone), thigh (femur), leg (patella, tibia, and fibula), and the foot (calcaneus, cuboid, 3 cuneiforms, 5 metatarsals, navicular, 14 phalanges, and talus). Each of the groups was applied a rigid material type. The thin shell elements were given a uniform unity thickness and the density of the elements were adjusted so that the mass of a segment would match that of a 50th percentile [10]. Additionally a 40 kg (88.2 lb.) point pass was positioned at the top of the pelvis to simulate the upper portion of the body in order to maintain the inertial influences of the body. With the material properties and mesh applied, the leg was positioned into an average vehicle occupant's sitting position [10]. Figures 1 displays the finite element mesh of the leg in the seated position and Figure 2 displays a rendered isometric view of the leg with the joints' axis of rotation shown.

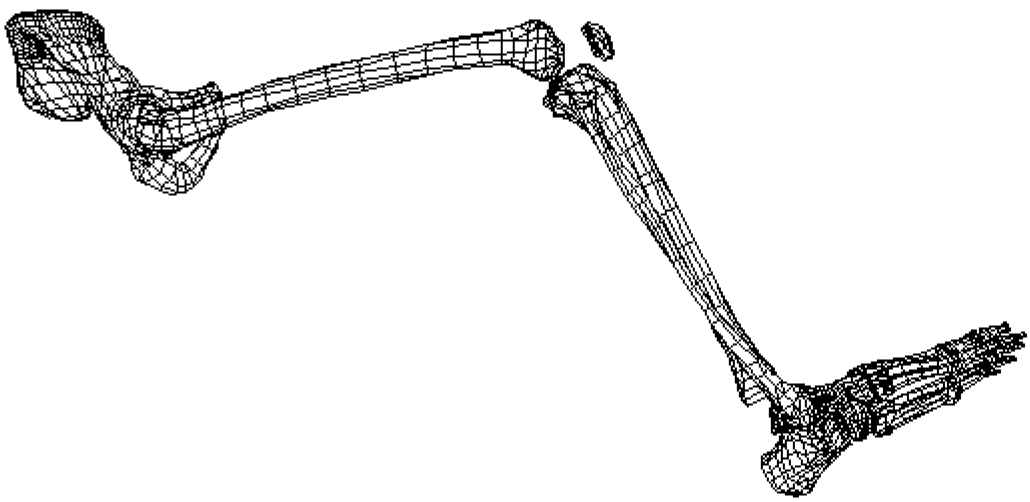

Figure 1: Finite element mesh of lower extremity model in vehicle occupant seated position

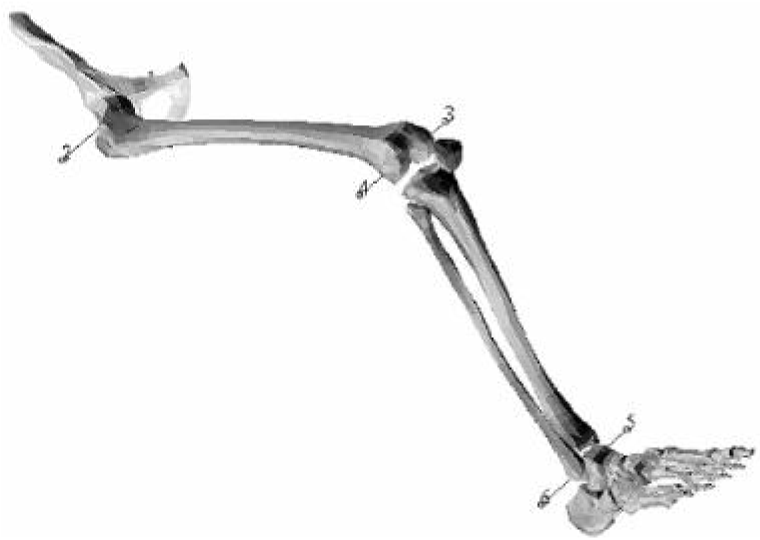

Figure 2: Isometric view of the seated leg with the axis of rotation for each joint displayed

The model was translated into an input deck for LS-DYNA3D version 930 [11]. The joints were defined with non-linear load curves for the stiffness and damping being applied to the three respective joints. The load curves are in the form of joint angle vs. stiffness moment and rate of rotation vs. damping moment following Equation 1.

This study was to determine the effects of muscle tensioning on the joints in the lower limb during a high deceleration event and investigate the injury potential to the ankle in such a case. With this in mind, it was necessary to apply the external loading conditions in order to simulate a high speed impact event. A seat belt was added in the form of a parallel spring and damper connecting the pelvis and a newly defined belt anchor. The element constants for the seat belt were K=6.0104 N/m for the spring and C=1000 N·s/m for the damper. The simulated crash pulse was of the NCAC's simulation of NHTSA Test #1400, a Taurus to Taurus head on collision, at 35 mph each, with a 50% overlap [12]. The seat belt, belt anchor, and the leg were given an initial velocity of 56 km/hr (35 mph). For the impact event, at time t=0, the belt anchor was applied the velocity profile of the car's center of gravity while the velocity profile of the toepan was input to the foot. The total simulation time is 150 ms. For test run #1400 there is a maximum toepan intrusion of 40 mm horizontally. All data taken from the Taurus-Taurus run was filtered using a standard SAE 60 Hz filter.

To study muscle tensioning effects, a joint could be in one of three states: passive only, passive and 50% active, or passive and 100% active. Three joints, with three possible joint conditions each, results in a possibility of 27 combinations in which the joints could be loaded from internal torques. The values for 100% activation were taken from Gordon *et al*. [4] and the values for 50% activation were simply scaled from the 100% values. Figure 3 displays the three combinations of ankle joint activation and the corresponding angle vs. moment curve for each. The investigation was to compare results such as joint position, joint moments, and other reactive forces to determine which combinations of muscle activity were potentially harmful.

Results

Comparisons between joint angle, joint moment, and muscle activation level were made. It was previously stated that joint angle is the best indicator of injury for loading the ankle in dorsiflexion, therefore, injury predictions could be made by comparing joint angles to the failure levels found experimentally.

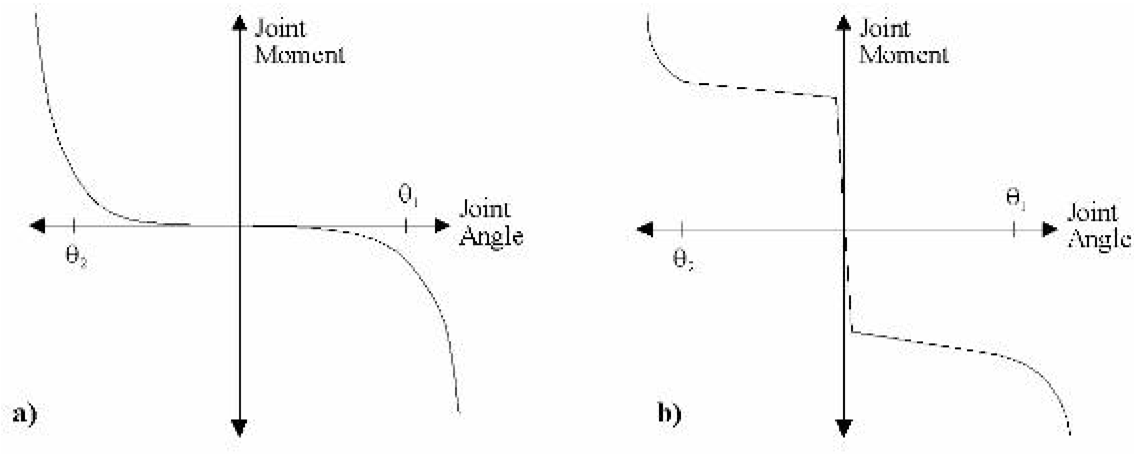

Figure 3: Ankle joint angle vs. stiffness moment for
a) passive activation only, b) 100% muscle activation.

Table 3: Maximum dorsiflexion angle and
corresponding ankle joint moment for each test case.

Test #	Max. Angle [degrees]	Moment [N-m]
111	55.2	40.6
112	12.1	27.1
113	18.3	81.6
121	59.7	60.4
122	12.2	27.4
123	16.6	73.9
131	61.7	77.0
132	13.3	30.0
133	15.1	60.8
211	61.8	77.6
212	25.2	58.0
213	18.7	83.3
221	63.4	102.0
222	26.7	61.5
223	16.9	75.2
231	62.8	92.4
232	28.6	66.4
233	15.2	67.3
311	62.1	81.9
312	44.7	113.0
313	17.7	78.6
321	63.5	106.0
322	45.0	115.0
323	15.3	68.1
331	64.2	120.0

332	45.1	115.0
333	13.0	57.5

There were 27 different simulations run. For each test run, the maximum angle of the ankle and the corresponding moment at this angle are found in Table 3. The test number contains three numbers. The first represents the hip, the second the knee, and the third the ankle. Since a joint could have one of three levels of activation a number 1 corresponds to passive only, a 2 corresponds to passive and 50% active muscles, and a 3 corresponds to passive and 100% active muscles. For example, test run number 1-2-3 indicates that the hip is passive only, the knee is passive and 50% active, and the ankle is passive and 100% active.

There was a large spread on the results and some noticeable trends formed. The angle in dorsiflexion ranged from 12.1° to 64.2° . Some trends that were noticed involving joint angle and subsequent injury potential include:

4. The highest values for joint angle occurred in cases in which the ankle was constrained only by passive joint torques.
5. Increasing the activation level in the ankle decreased the maximum angle of dorsiflexion in the ankle.
6. Increasing the activation level in the hip increased the maximum angle of dorsiflexion in the ankle.
7. The effects of tensing the knee had no distinct pattern of results in ankle joint angle.
8. When the ankle was only passively activated, the peak dorsiflexion angle occurred early in the impact event, between 45 and 70 ms.
9. When the ankle was only passively activated, a second sharp increase in dorsiflexion was noted around 125 ms.
10. When the ankle was 50% or 100% activated, the peak dorsiflexion angle occurred later in the impact event, between 110 and 120 ms.
11. The point of maximum dorsiflexion was successively followed by the peak value in plantarflexion as the ankle swiftly rotated back

Ankle joint moment ranged from 27.1 to 120.0 N·m. Ankle joint moment did not have a direct correlation with joint angle but it did correlate to the tensing patterns of the joints. As the level of activation remained constant in the ankle and the other joints were gradually stiffened, the moment in the ankle joint rose sharply. From case 1-1-1 to case 3-1-1 the moment in the joint nearly tripled from 40.6 to 120.0 N·m.

Crash Investigation Methodology

Application of a computer model to investigate injuries in a crash requires detailed and precise documentation of the vehicle and injured occupant. The documentation required by a NASS case provides a baseline for the methodology. Additional protocols have been developed to collect data on the occupant and the vehicle. These new protocols are implemented and refined by the interdisciplinary team at the William Lehman Injury Research Center.

With regard to the occupant, extensive additional data is collected. Externally visible injuries and abrasions are photographed at the hospital. The lengths of limbs are measured and documented. An interview determines the normal seating position, handiness, footwear, and extent of bracing or braking actions. Injuries are further documented in the case file by the inclusion of X-rays, CT scans, MRI's. bone density scans, external photos, injury diagrams, a clinical description of treatment, response, and outcome.

With regard to the vehicle, additional attention is given to the geometry of the interior and the position of the occupant - particularly the lower extremities. A protocol has been developed to measure and document the vehicle interior geometry, including footwell and knee restraint intrusion. Seat location is assessed based on physical evidence and information from the interview. The position of the upper body and lower limbs is estimated initially by locating a skeletal device of the lower extremity based on physical evidence. The location is further confirmed by interdisciplinary examination of the injuries and the forces which produced them. In some cases, preliminary reconstruction of the occupant kinematics is made, using crash films and a lumped mass computer model.

Documenting Vehicle Interior Geometry

The computer model requires accurate documentation of geometry of any vehicle interior components which influence the occupant kinematics. The protocol for interior measurements builds on the method developed for measuring external damage which is routinely applied by NASS investigators.

Figure 4 shows the equipment used by NASS investigators for external damage measurement. The protocol requires measurement of damage relative to the plane of the undamaged vehicle. Measurements are taken at six equally spaced locations across the damaged area.

Figure 4: NASS protocol for external damage measurement.

The interior geometry documentation requires similar measurements, but requires profile measurements at each of the six locations. In concept, the profile measurements document the configuration of the interior in a series of vertical planes at specified locations across the vehicle.

A computer generated illustration of vehicle interior measurements is shown in Figure 5. The measurements are made at the intersections of the surfaces which represent the floor, toe pan, fire wall, knee restraint, dash board, etc. The seat, steering wheel and brake pedal are represented by locating the edge of the surfaces. A minimum of six vertical planes are required to document the interior of the driver position. These planes are located as follows: the outside edge of the left foot rest; the inside edge of the left foot rest; the center of the steering wheel; the center of the brake pedal, the left lower edge of the floor hump, and the left upper edge of the floor hump. In addition measurements to document brake pedal width, steering wheel width, and seat belt anchorage locations is required.

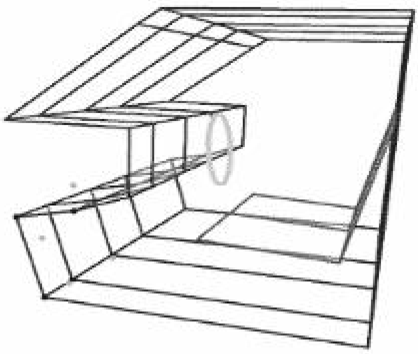

Figure 5: Wireframe representation of undeformed vehicle interior comprised of six vertical measurement planes.

If intrusion of the interior is present, two sets of measurements are required. One set is required on the damaged interior, and one on an identical undamaged vehicle.

Measurements on two different vehicles requires the establishment of a common Reference Point. The Reference Point must be in an area of the vehicle which has not sustained permanent deformation. For frontal crashes, the upper corner of the driver's door opening is often a convenient Reference Point.

Figures 6 and 7 show a crash investigator establishing a Vertical Reference Plane (Y-Z Direction) relative to the door opening Reference Point.

Figure 7 also shows a secondary measuring plane (Y-Z direction) defined by the two vertical measuring rods against the dashboard. This plane is positioned near the dashboard, permitting convenient measurements of the dashboard and footwell area.

Figure 6: Vertical reference frame determination relative to door opening.

Figure 7: Secondary reference plane determination.

Figures 8 and 9 show the measurements required to locate the measuring plane (Y-Z Direction). The Measuring Plane (Y-Z Direction) is parallel to the Vertical Reference Plane (Y-Z Direction) and at a distance which is recorded.

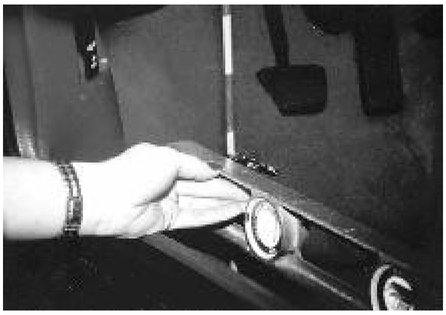

Figure 8: Measurements near footwell to locate measuring plane

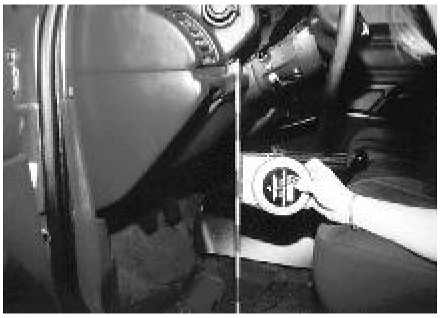

Figure 9: Measurements near dashboard to locate measuring plane.

Six interior Coordinate Planes (X-Z Direction) are established in locations across the interior as described earlier. Figures 10 and 11 show measurements to locate the outermost Coordinate Plane (X-Z Direction) relative to the undeformed vehicle exterior. Other Coordinate Planes (X-Z Direction)are located parallel to the outermost plane at a known distance.

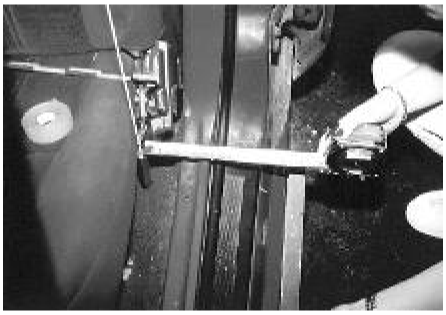

Figure 10: Measurements to locate the outermost coordinate plane near seatbelt anchor point.

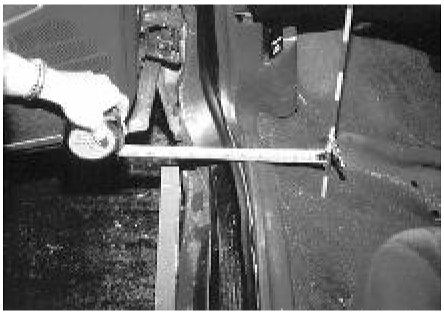

Figure 11: Measurements to locate the outermost coordinate plane near door hinges.

Figure 12 shows a measurements of the X and Z coordinates in the Coordinate Plane (X-Z Direction) at the lower edge of the floor hump. The measurement is relative to the Measuring Plane (Y-Z Direction).

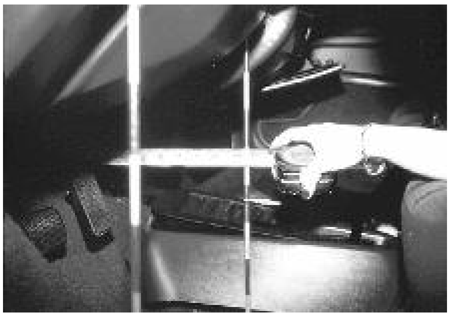

Figure 12: Measurement of X and Z in the Coordinate Plane.

The three dimensional coordinates of the anchor points of the seat belt anchors are measured relative to the Reference Plane, as shown in Figure 13.

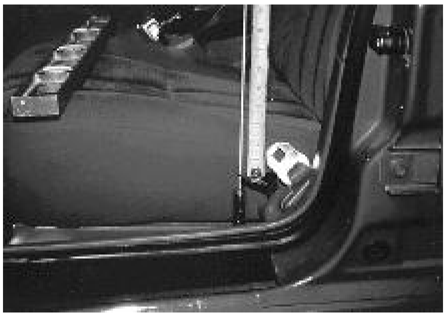

Figure 13: Measurement of three dimensional coordinates of seatbelt anchor point.

A computer program has been developed which plots the interior geometry of the vehicle from the data points. The image can be enhanced to show intrusion as seen in Figure 14. The input data for the computer image is stored as part of the case file.

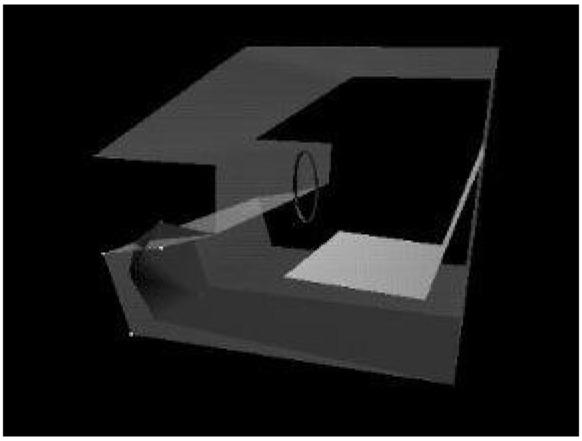

Figure 14: Computer generated image of deformed vehicle interior showing intrusion.

Positioning of Lower Limbs in the Vehicle

The location of lower limbs in the vehicle is initially based on physical evidence. Interior damage from body contacts, skin transfers and other witness marks are noted. Pictures of abrasions to the occupant are also considered. The use of a skeletal device of the human lower extremity is also helpful in establishing leg position.

A typical application of the methodology is illustrated in Figures 15 and 16.

Figure 15: Abrasions found on drivers leg.

Figure 15 shows abrasions on the leg of a driver with ankle injuries. Matching skin transfers were found on the lower edge of the right facia in the footwell area.

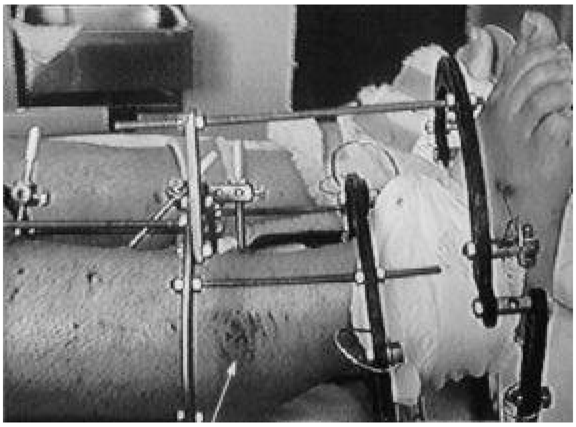

Figure 16: Skeletal device representing drivers leg.

Figure 16 shows the skeletal device adjusted to the length of the injured drivers legs, and placed so the abrasions match the skin transfer locations. Final location is determined by considering alternative locations from positioning the device and from considering the forces which produced the injury.

Discussion

The approach outlined offers an unconventional technology for studying the causes of ankle injuries. The combination of detailed accident investigation with the evaluation of the influence of crash parameters using computer models requires sophistication in both areas. However, the approach underway applies no more sophistication than needed.

Although the model presented here is rather elementary, it did demonstrate the feasibility of analyzing muscle tensioning effects and injury potential in low level models. The above work intended to focus on the developmental process of this finite element model of the lower extremity. It is probably best to first discuss the limitations of this model and how these limitations will effect the results. These limitations include:

In simulating the external loading from the crash pulse on the leg, there was no interaction will the vehicles interior. Loading on the ankle will be different if the knee impacts and crushes into a knee bolster. This effect will be to essentially lock the knee and hip in place, subsequently loading the ankle more aggressively. Other concerns are secondary impacts with the foot space and pelvic interactions with the seat cushions.

There is no failure associated with this level of model; therefore, when the joint reaches injury levels it will always "spring" back. When the stiffness in the joint causes this spring back, the foot is likely to move too extremely in the opposite direction. This response is likely the cause of the large values of plantarflexion following each peak in dorsiflexion.

There is no active damping in the joints for cases of high muscle tensioning. This causes a "ringing" effect and an oscillatory response when loaded. Human joints will rapidly damp out these effects.

Joints were only permitted to move in one plane, therefore, all forces and loading were not distributed through a joints entire range-of-motion. Motions such as inversion-eversion in the ankle may account for some energy redistribution thus lowering injury potential.

Although these downfalls are inherent in this model, they do not detract from the purpose of its creation and its use as a preliminary analysis tool. The model demonstrated, that even at low levels of detail, muscle tensioning greatly effects the kinematics of the lower extremities under impact loading. By producing such a wide range of angles and moments it is most definitely an issue that must be addressed when discussing safety and design. The model also demonstrated the ease to which muscle tensioning can be incorporated into finite element models. Other human surrogates have a much more difficult time to do this. Dummies need adjustable joints and subsequent recalibration while cadavers require some form of joint locking device.

Validation of a three dimensional model is now underway. This model will be useful in studying conditions with non-frontal acceleration components and intruding toepans. Longer term, research is underway to incorporate the muscles, with attachments at appropriate locations. The result should be an improvement in the simulation of load paths within the lower limbs. In the meantime, useful ankle injury studies will be undertaken with the model at its current stage of development.

Conclusions

Concerning the results, some conclusions can be made from this parametric study. These include:

- The ankle showed the highest level of injury potential when it was only passively tensed. Additionally, the peak values occurred early in the crash event (~ 50 ms). This indicates that the ankle joint is susceptible to injuries caused by rapid deceleration when the occupant is not aware of an oncoming collision. These peak levels can not be associated with toepan intrusion because that occurs after 100 ms. It must be noted that it is highly unlikely for the ankle to be only passively activated. The simple nature of operating an automobile requires some form of muscle tension through pedal or toepan interactions.

- Higher levels of ankle loading were seen when the other joints were tensed. The leg can be viewed as a jointed beam. It makes sense that the weakest joint will have to absorb most of the loading applied, because, this load will be transmitted across stiff joints. Stiffening of the hip joint had the greatest effects on the ankle. For cases when an oncoming collision is apparent to the driver, braking is applied most readily through a rapid extension of the leg at the hip and knee. This action leaves the ankle more susceptible to increased loading.
- For cases in which the ankle was tensed, the peak loading occurred around 110 ms. This is the same time at which toepan intrusion occurs in this simulation. In these runs (50% or 100% ankle tension), the intrusion showed to be the greatest contributor to ankle loading.
- The model has demonstrated it's potential has a safety research tool; therefore, it is necessary to develop this model to the next level. The most immediate changes will involve the incorporation of three dimensional joints for complete joint articulation. By incorporating these joints, additional data is needed for passive and active stiffness characteristics for motion out of the sagittal plane. Additionally, geometry can be added to represent the mass of the soft tissues encompassing the skeletal structures. This outer surface will provide a contact surface for the lower limb for interactions with an occupant compartment interior. Finally, the addition of material models representing the various biological tissues will make this model one of the most detailed and useful human surrogates for lower extremity impact studies. The approach should maintain a ground-up methodology with more detail being added to the existing model at each stage. With this method, the model will remain useful at each stage and will not require complete redevelopment each time more detail is desired.

References

12. Thomas, P., and Bradford, M. "A Logistic Regression Analysis Of Lower Limb Injuries," *Proceedings of the 39th Annual AAAM,* (1995), pp. 287-310.

13. Malliaris, A. C., "Lower Extremity Injuries In Car Crashes," FHWA/NHTSA National Crash Analysis Center Report (May 1995).

14.Marieb, E. N., Human Anatomy and Physiology, (1992) ISBN No. 0-8053-4120-X, Benjamin - Cummings Publishing Company, Inc., Redwood City, California.

15.Audu, M. L., and Davy, D. T., "The Influence of Muscle Model Complexity in Musculoskeletal Motion Modeling," *Journal of Biomechanical Engineering*, (May 1985) vol. 107, no. 5, pp. 147-157.

16.Yamaguchi, G, "Kinematic Models of Joints and Musculotendon Actuation," *Movement Biomechanics: Course Notes*, (1993) Arizona State University, Tempe, Arizona.

17.Gordon, S. L., Orticke, P. N., Prince, J., and McMeekin, R. R., "Dynamic Characteristics of the Human Leg Joints," *Proceedings of the 21st Stapp Car Crash Conference*, (1977) SAE Technical Paper No. 770924, pp. 419-441.

18.Begeman, P. D., and Prasad, P., "Human Ankle Impact Response in Dorsiflexion," (1990) SAE Technical Paper No. 902308. Reprinted in Hybrid III: The First Human-Like Crash Test Dummy, SAE PT-44, 1994.

19.Crandall, J.R., Dekel, U., Hall, G.W., Schreiber, P., and Pilkey, W.D., "The Effects of Lower Extremity Boundary Conditions on Ankle Responses During Rotation Tests," (November 1995) An informal presentation based on ongoing research, *23rd International Workshop on Human Subjects for Biomechanical Research*, San Diego, California.

20.Viewpoint DataLabs - Database Catalog, Viewpoint DataLabs, 625 South State Street, Orem, Utah, 84058, Phone 801-229-3000, FAX 801-229-3300.

21.Robbins, D. H., "Anthropomorphic Specifications for Mid-Sized Male Dummy," (December 1983), Transportation Research Institute Report No. UMTRI-83-53-2, United States Department of Transportation, National Highway Traffic Safety Administration Contract No. DTNH22-80-C-07502, Washington, D.C.

22.Hallquist, J. O., LS-DYNA3D User's Manual: Version 930, (1994) Livermore Software Technology Corporation, Livermore, California.

23.Reichert, R., Validation of a Ford Taurus Finite Element Model for Frontal Offset Impacts, (1995) Master's Thesis, The George Washington University, Washington, D.C.